CONF-810203--13

SOLIDIFICATION BEHAVIOR AND MICROSTRUCTURAL ANALYSIS

OF AUSTENITIC STAINLESS STEEL LASER WELDS*

MASTER

S. A. David and J. M. Vitek

Metals and Ceramics Division
Oak Ridge National Laboratory
Oak Ridge, Tennessee 37830

Solidification behavior of austenitic stainless steel laser welds has been investigated with a high-power laser system. The welds were made at speeds ranging from 13 to 60 mm/s. The welds showed a wide variety of microstructural features. The ferrite content in the 13-mm/s weld varied from less than 1% at the root of the weld to about 10% at the crown. The duplex structure at the crown of the weld was much finer than the one observed in conventional weld metal. However, the welds made at 25 and 60 mm/s contained an austenitic structure with less than 1% ferrite throughout the weld. Microstructural analysis of these welds used optical microscopy, transmission electron microscopy, and analytical electron microscopy. The austenitic stainless steel welds were free of any cracking, and the results are explained in terms of the rapid solidification conditions during laser welding.

*Research sponsored by the Division of Materials Sciences, U.S. Department of Energy, under contract W-7405-eng-26 with the Union Carbide Corporation.

DISCLAIMER

Introduction

Austenitic stainless steels form an important class of engineering materials in several energy systems. A significant problem in the production of fully austenitic stainless steel welds is their tendency for hot cracking. To minimize this tendency, the compositions of welding materials are generally modified to produce small amounts of δ-ferrite in the as-welded microstructure. For example, in type 308 stainless steel weld metal, ferrite contents of 5 to 10% are common. Although ferrite has been found to effectively prevent hot cracking (1–3), it also leads to corrosion susceptibility and embrittlement at elevated temperatures. Hence, it would be highly desirable to produce fully austenitic stainless steel welds without the tendency to hot crack.

Extremely high cooling rates have produced unusual microstructures in austenitic stainless steels containing duplex structures (4). However, neither were these microstructures characterized fully nor were their origins understood. The purpose of our work is to characterize austenitic stainless steel laser welds and understand the observed modifications in microstructure.

Experimental Procedure

A multipass conventional weld overlay of type 308 stainless steel filler metal [20.5 Cr, 10.5 Ni, 1.5 Mn, 0.44 Si, 0.065 C, 0.022 P, 0.008 S, balance Fe (wt %)] was made on a 12-mm-thick plate of type 304L stainless steel; see Figure 1. The resultant block of type 308 stainless steel overlay was approximately 12 mm high, 25 mm wide, and 150 mm long. Autogenous laser welds (melt runs) were made on this overlay at welding speeds of 13, 25, and 63 mm/s. The welds were made with an AVCO multikilowatt continuous-wave CO_2 laser system with an output of 9 kW, in the annular beam mode. During welding, shielding was provided by helium gas flowing through an off-axis diffuser at 5.6 m^3/h.

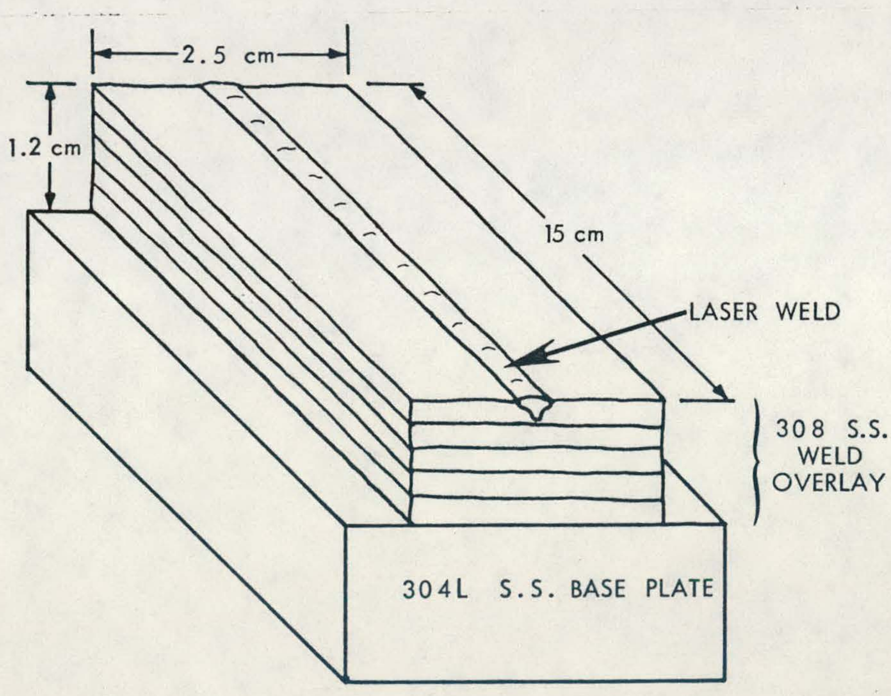

Fig. 1 - Schematic of the weld pad used for the laser weld experiment.

Microstructural analysis of these welds was performed by using optical microscopy, transmission electron microscopy, and analytical electron microscopy. For optical microscopy the samples were etched with a solution containing five parts concentrated HCl to one part concentrated HNO_3. Foils of weld metal for electron microscopic analysis were electropolished with a dual-jet polishing apparatus and a solution of sulphuric acid in methanol (1:7). Most of the electron microscopy was performed at 120 kV.

Results and Discussion

A typical microstructure of type 308 stainless steel weld produced by one of the conventional welding processes, namely gas tungsten arc (GTA), is shown in Figure 2. The photomicrograph shows the vermicular and lacy

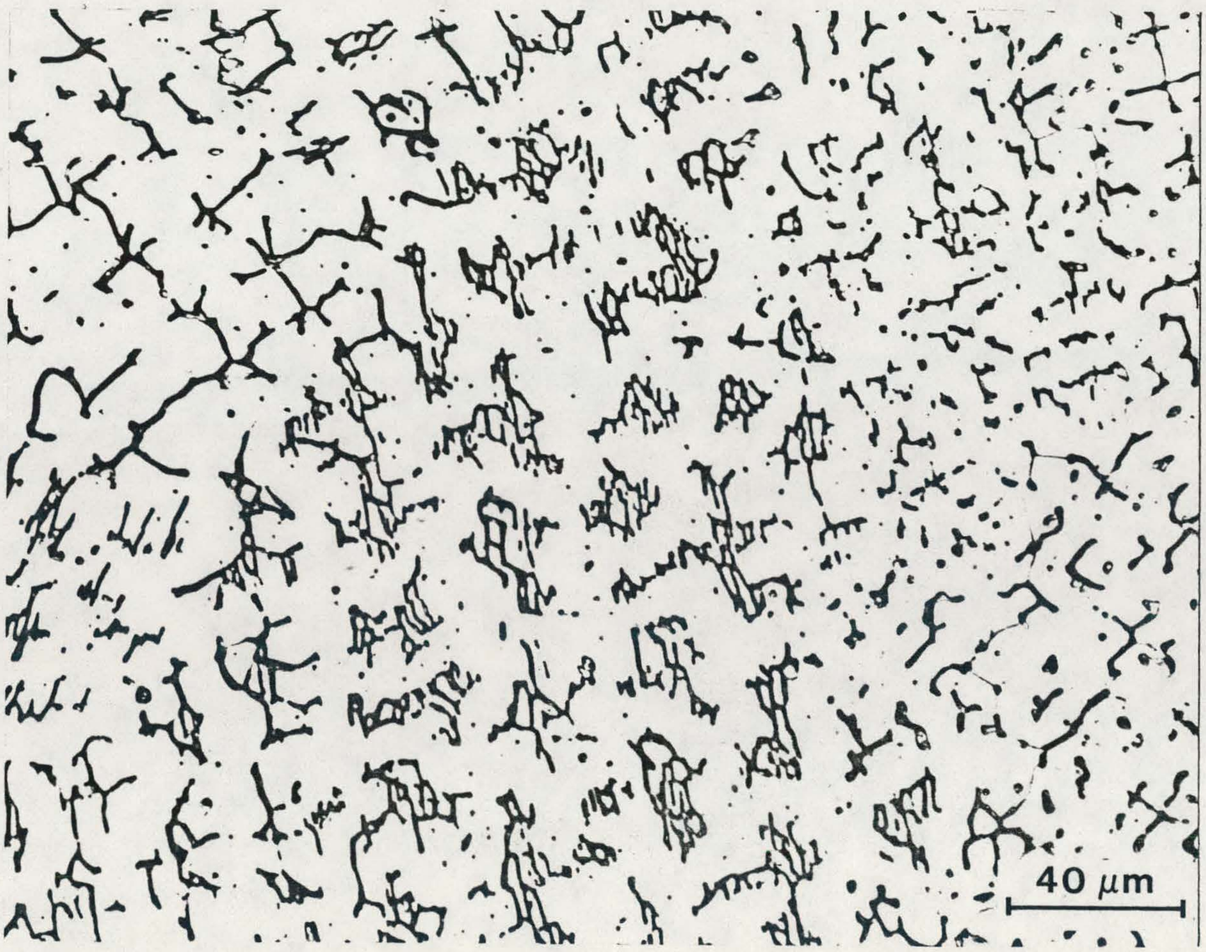

Fig. 2 - A gas tungsten arc bead-on-plate weld. Type 308 stainless steel filler metal.

ferrite forms in austenite. An earlier study (5) revealed that the solidification sequence in type 308 stainless steel weld metal consists of the primary crystallization of δ-ferrite with subsequent envelopment by austenite and a $\delta \rightarrow \gamma$ transformation continuing below the solidus, leaving behind a skeletal network of residual δ-ferrite. This particular ferrite has been shown (6) to be located along the cores of the primary and secondary dendrite arms. Sometimes the primary δ-ferrite formed during solidification may transform to Widmanstätten austenite at lower temperatures, leaving behind residual ferrite in acicular or lacy form. The ferrite in this case has been shown to be located within the primary cells or dendrites. These two modes of ferrite formation account for the origin of δ-ferrite in austenitic stainless steel welds containing duplex structures.

Macroscopic views of cross sections from the three laser welds are shown in Figure 3. In contrast to the type 308 stainless steel GTA weld,

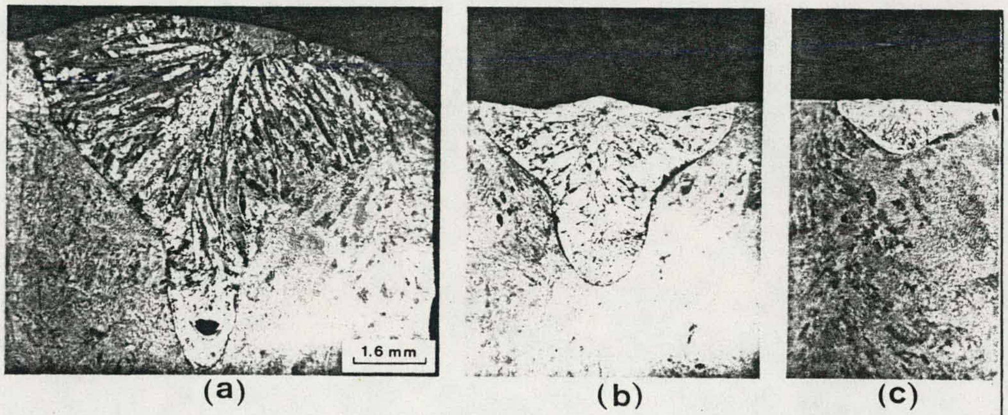

Fig. 3 - Macrostructure of the laser welds made at (a) 13, (b) 25, and (c) 63 mm/s.

laser welds of the same material obtained at welding speeds of 25 and 63 mm/s produced an almost fully austenitic structure with less than 1% ferrite. The ferrite is in the intercellular or interdendritic regions, suggesting a primary austenitic mode of solidification. Unlike the other fully austenitic stainless steel welds, these laser welds did not show any hot cracking tendency. Optical microscopy also revealed the presence of a third phase uniformly distributed within the weld metal, as shown in Figure 4. Figure 5 shows the 13-mm/s laser weld with a wide

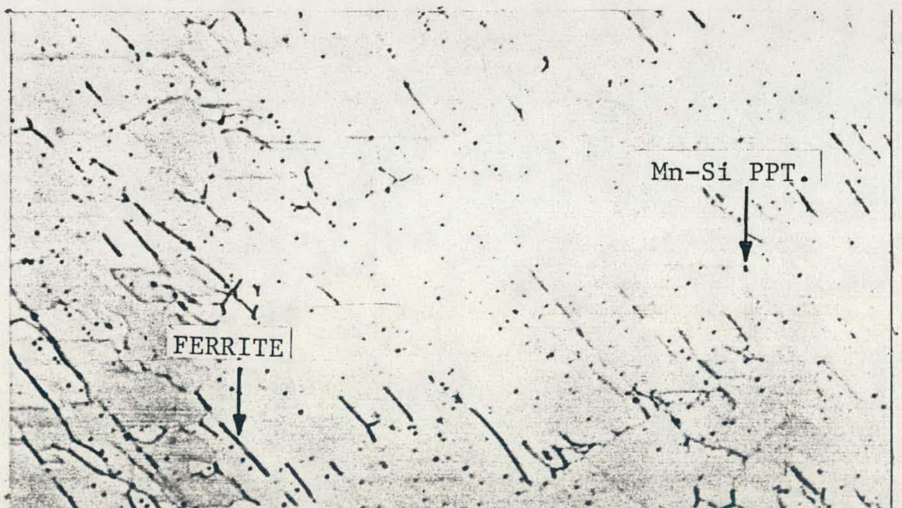

Fig. 4 - Photomicrograph showing intercellular ferrite and uniform distribution of third-phase particle identified as MnSi. Laser weld 25 mm/s.

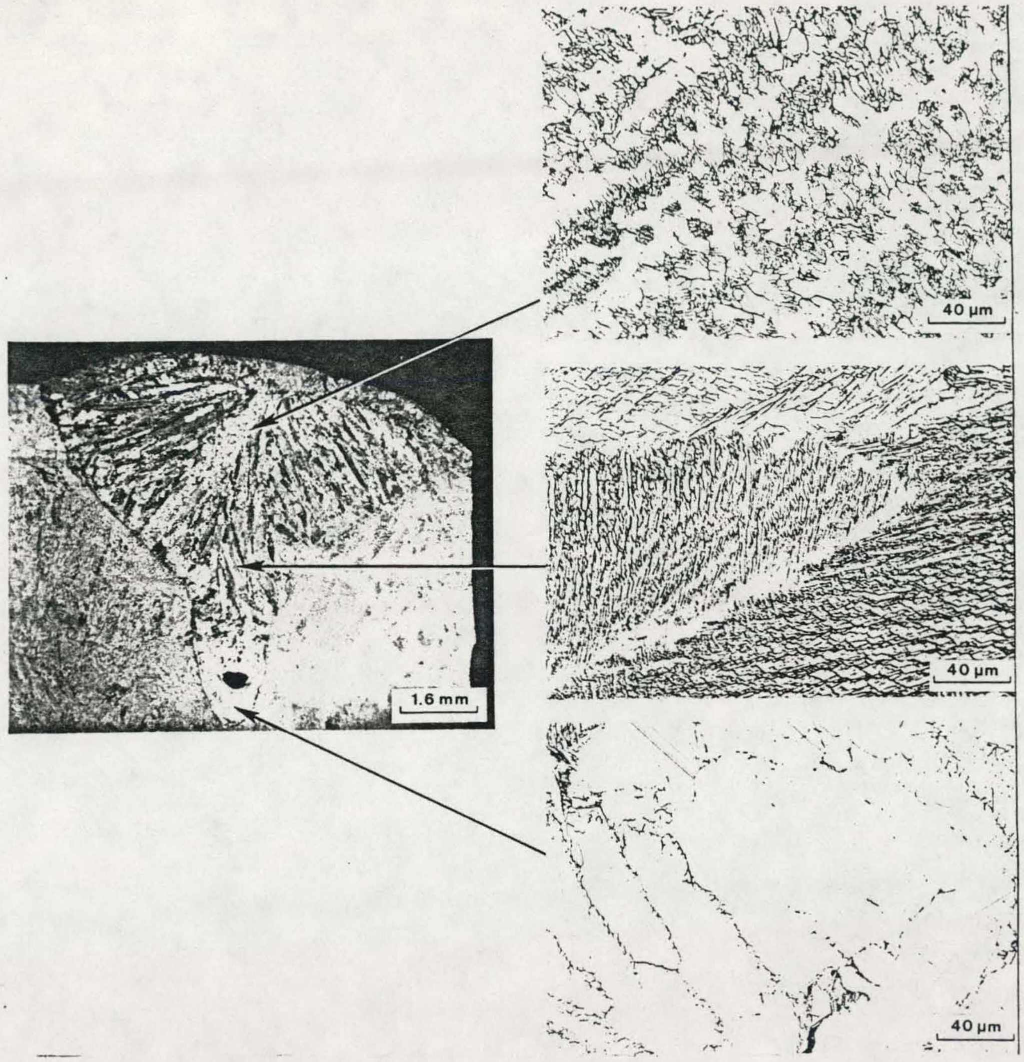

Fig. 5 - Variations in microstructure from root to the crown of the 13-mm/s laser weld.

variety of microstructures ranging from fully austenitic microstructure at the root of the weld to $\delta + \gamma$ duplex structure at the crown. The fully austenitic structure at the root of the weld may be attributed to the high cooling rates encountered in that part of the weld during welding. Mid-sections of the weld revealed a very fine duplex structure. The crown of the weld also contained a duplex structure of austenite and ferrite but coarser.

The origin of the fully austenitic structure in the laser welds is an interesting phenomenon that needs further investigation and understanding. Figure 6 shows the details of the microstructure along the fusion line of the laser weld made at 25 mm/s. Close examination revealed a change in the mode of solidification for type 308 stainless steel from primary ferrite, as seen commonly, to primary austenite. The presence of intercellular or interdendritic ferrite is further evidence of such a change in the mode of solidification. This may be rationalized as due to the excessive undercooling at the tip of the primary δ-ferrite cells or dendrites that could have changed the mode of solidification from primary δ-ferrite to primary austenite. A later paper will present a more extensive analysis of this result.

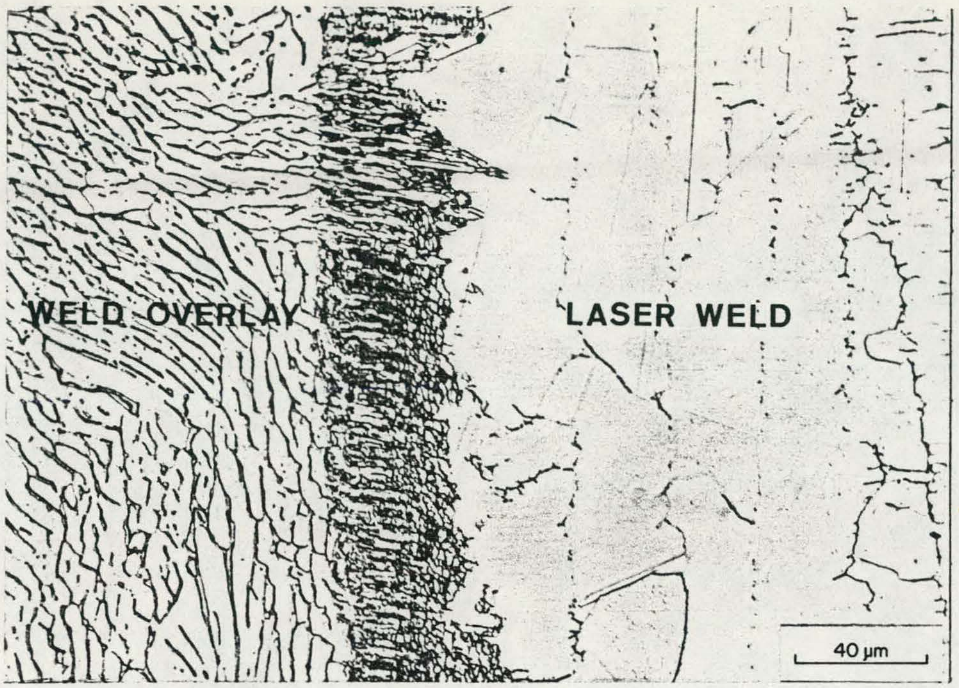

Fig. 6 - Fusion line of the 25-mm/s laser weld.

A transmission electron micrograph of a fully austenitic laser weld, Figure 7, shows the third-phase particles to be 100 to 200 nm in diameter. It also shows the presence of intercellular or interdendritic ferrite at high magnification. These particles contained mostly Mn and Si in addition to small amounts of Cr, Al, S, and Ti. A typical energy-dispersive x-ray spectrum for these particles is shown in Figure 8(b). The copper peak in the spectrum is due to the copper grid on which the

Fig. 7 - Typical transmission electron micrograph of the laser weld showing intercellular ferrite and MnSi particles.

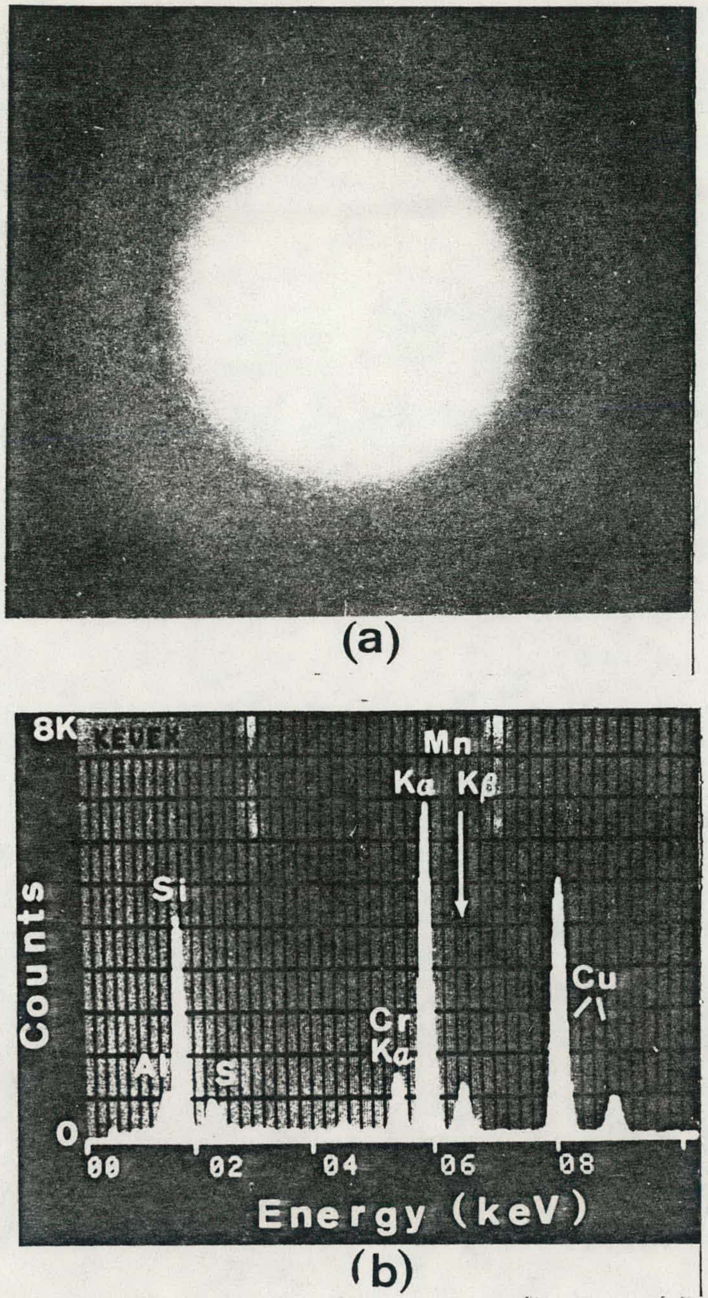

Fig. 8 - Third-phase particles observed in the laser welds made at 25 and 63 mm/s. (a) Microdiffraction pattern. (b) Typical energy spectrum.

replica was mounted for analysis. A microdiffraction technique, Figure 8(a), showed that these particles were amorphous. No evidence for these manganese- and silicon-rich particles was found in the conventional weld overlay. Spherical manganese- and silicon-rich particles have been observed elsewhere (7,8) and have been identified as oxide inclusions. In the present work, ascertaining the presence of oxygen in these particles was beyond the capability of the analytical instrument. Further work is under way to better understand the origin and nature of these particles.

Conclusions

Rapid cooling encountered during laser welding of type 308 stainless steel changed the mode of solidification from primary δ-ferrite to primary austenite. The resulting weld metal contains a very small amount of intercellular or interdendritic ferrite and the weld metal showed no sign of cracking. In addition to the presence of a very small amount of residual ferrite, a very fine and uniform distribution of third-phase particles was found in the weld metal and identified as amorphous and rich in manganese and silicon.

Acknowledgments

The authors gratefully acknowledge C. J. McHargue, Program Manager, for encouragement and support, L. B. Spiegel of AVCO Metal Working Lasers for making the welds and C. P. Haltom and W. H. Smith for metallography and electropolishing, respectively. The authors would like to acknowledge G. M. Goodwin and C. T. Liu for reviewing the manuscript and technical discussion. The manuscript was edited by S. Peterson and the camera-ready copy was prepared by A. F. Rice.

References

1. F. C. Hull, "Effect of Delta Ferrite on the Hot Cracking of Stainless Steel," Welding Journal (Miami), 46 (9) (1967) pp. 399-s–409-s.
2. J. C. Borland and R. N. Younger, "Some Aspects of Cracking in Austenitic Steels," British Welding Journal, 7 (1) (1960) pp. 22–60.
3. Y. Arata, F. Matsuda, and S. Katayama, "Solidification Crack Susceptibility in Weld Metals of Fully Austenitic Stainless Steel (Report 1) — Fundamental Investigation on Solidification Behavior of Fully Austenitic and Duplex Microstructures and Effect of Ferrite on Microsegregation," Transactions of JWRI, 5 (2) (1976) pp. 35–51.
4. W. T. DeLong, "Ferrite in Austenitic Stainless Steel Weld Metal," Welding Journal (Miami), 53 (7) (1974) pp. 273-s–286-s.
5. S. A. David, G. M. Goodwin, and D. N. Braski, "Solidification Behavior of Austenitic Stainless Steel Filler Metals," Welding Journal (Miami), 58 (11) (1979) pp. 330-s–336-s.
6. S. A. David, "Ferrite Morphology and Variations in Ferrite Content in Austenitic Stainless Steel Welds," Welding Journal (Miami), 60 (4) (1981) pp. 63-s–71-s.
7. K. W. Mahin, Characterization of Ferritic G.M.A. Weld Deposits in 9% Ni Steel for Cryogenic Applications, Ph. D. Thesis, University of California, Berkeley, 1980; also issued as Lawrence Berkeley Laboratory Report LBL-10922.
8. S. R. Keown and R. G. Thomas, The Role of Delta Ferrite in the Thermal Aging of Austenitic Weld Metals, Central Electricity Generating Board (England) Report RD/M/R299, 1980.